Cascaded SRS of single- and double-scale fiber laser pulses in long extra-cavity fiber

Sergey Kobtsev,[1,2,*] Sergey Kukarin,[1,2] Sergey Smirnov,[1,2] and Ilya Ankudinov[1]

[1]*Division of Laser Physics and Innovative Technologies, Novosibirsk State University, Pirogova str., 2, Novosibirsk 630090, Russia*

[2]*"Tekhnoscan-Lab" LLC, Inzhenernaia str., 26, Novosibirsk, 630090, Russia*

[*]*kobtsev@lab.nsu.ru*

Abstract: This work presents, for the first time, the results of studies of stimulated Raman scattering (SRS) in 1.2-km P_2O_5-doped silica fiber of radiation of single- and double-scale picosecond pulses generated in a fiber master oscillator and amplified in a one-stage fiber amplifier. Shown are differences in supercontinuum spectra composed of several Stokes components when pumped with pulses of different structure. More efficient Raman transformation of double-scale pulses was identified, leading to broader supercontinuum spectra.

OCIS codes: (190.5650) Raman effect; (190.5890) Scattering, stimulated; (060.4370) Nonlinear optics, fibers; (140.4050) Mode-locked lasers; (140.3510) Lasers, fiber.

References and links

1. M. Fermann, *Nonlinear polarization evolution in passively modelocked fiber lasers* (Compact Sources of Ultrashort Pulses, I. N. Duling (Ed.), Cambridge University, 1995), Chap. 5.
2. N. Akhmediev and A. Ankiewicz, *Solitons, Nonlinear Pulses and Beams* (Chapman and Hall, 1997).
3. J. M. Soto-Crespo, P. Grelu, N. Akhmediev, and N. Devine, "Soliton complexes in dissipative systems: Vibrating, shaking, and mixed soliton pairs," Phys. Rev. E Stat. Nonlin. Soft Matter Phys. **75**(1), 016613 (2007).
4. S. Chouli and P. Grelu, "Rains of solitons in a fiber laser," Opt. Express **17**(14), 11776–11781 (2009).
5. B. Oktem, C. Ülgüdür, and Ö. Ilday, "Soliton-similariton fibre laser," Nat. Photonics **4**(5), 307–311 (2010).
6. S. V. Smirnov, S. M. Kobtsev, S. V. Kukarin, and S. K. Turitsyn, *Mode-locked fibre lasers with high-energy pulses* (Laser Systems for Applications, K.Jakubczak (Ed.), InTech, 2011), Chap. 3.
7. D. Mao, X. Liu, L. Wang, H. Lu, and L. Duan, "Coexistence of unequal pulses in a normal dispersion fiber laser," Opt. Express **19**(17), 16303–16308 (2011).
8. P. Grelu and N. Akhmediev, "Dissipative solitons for mode-locked lasers," Nat. Photonics **6**(2), 84–92 (2012).
9. W. H. Renninger, A. Chong, and F. W. Wise, "Pulse shaping and evolution in normal-dispersion mode-locked fiber lasers," IEEE J. Sel. Top. Quantum Electron. **18**(1), 389–398 (2012).
10. S. Smirnov, S. Kobtsev, S. Kukarin, and A. Ivanenko, "Three key regimes of single pulse generation per round trip of all-normal-dispersion fiber lasers mode-locked with nonlinear polarization rotation," Opt. Express **20**(24), 27447–27453 (2012).
11. W. H. Renninger and F. W. Wise, *Dissipative Soliton Fiber Lasers* (Fiber lasers, O. G. Okhotnikov (Ed.), Wiley-VCH Verlag GmbH & Co. KgaA, 2012), Chap. 4.
12. S. Wabnitz, "Optical turbulence in fiber lasers," Opt. Lett. **39**(6), 1362–1365 (2014).
13. M. Horowitz, Y. Barad, and Y. Silberberg, "Noiselike pulses with a broadband spectrum generated from an erbium-doped fiber laser," Opt. Lett. **22**(11), 799–801 (1997).
14. O. Pottiez, R. Grajales-Coutiño, B. Ibarra-Escamilla, E. A. Kuzin, and J. C. Hernández-García, "Adjustable noiselike pulses from a figure-eight fiber laser," Appl. Opt. **50**(25), E24–E31 (2011).
15. J. Li, Z. Zhang, Z. Sun, H. Luo, Y. Liu, Z. Yan, C. Mou, L. Zhang, and S. K. Turitsyn, "All-fiber passively mode-locked Tm-doped NOLM-based oscillator operating at 2-μm in both soliton and noisy-pulse regimes," Opt. Express **22**(7), 7875–7882 (2014).
16. S. Kobtsev, S. Kukarin, S. Smirnov, S. Turitsyn, and A. Latkin, "Generation of double-scale femto/pico-second optical lumps in mode-locked fiber lasers," Opt. Express **17**(23), 20707–20713 (2009).
17. B. Nie, G. Parker, V. V. Lozovoy, and M. Dantus, "Energy scaling of Yb fiber oscillator producing clusters of femtosecond pulses," Opt. Eng. **53**(5), 051505 (2014).
18. S. M. Kobtsev and S. V. Smirnov, "Fiber lasers mode-locked due to nonlinear polarization evolution: golden mean of cavity length," Laser Phys. **21**(2), 272–276 (2011).
19. I. A. Yarutkina, O. V. Shtyrina, M. P. Fedoruk, and S. K. Turitsyn, "Numerical modeling of fiber lasers with long and ultra-long ring cavity," Opt. Express **21**(10), 12942–12950 (2013).
20. S. V. Smirnov, S. M. Kobtsev, and S. V. Kukarin, "Efficiency of non-linear frequency conversion of double-scale pico-femtosecond pulses of passively mode-locked fiber laser," Opt. Express **22**(1), 1058–1064 (2014).

#214558 - $15.00 USD Received 23 Jun 2014; accepted 7 Aug 2014; published 20 Aug 2014

21. C. Headley III and G. P. Agrawal, "Unified description of ultrafast stimulated Raman scattering in optical fibers," J. Opt. Soc. Am. B **13**(10), 2170–2177 (1996).
22. S. M. Kobtsev and S. V. Kukarin, "All-fiber Raman supercontinuum generator," Laser Phys. **20**(2), 372–374 (2010).
23. H. Sayinc, K. Hausmann, U. Morgner, J. Neumann, and D. Kracht, "Picosecond all-fiber cascaded Raman shifter pumped by an amplified gain switched laser diode," Opt. Express **19**(27), 25918–25924 (2011).
24. H. Pourbeyram, G. P. Agrawal, and A. Mafi, "Stimulated Raman scattering cascade spanning the wavelength range of 523 to 1750 nm using a graded-index multimode optical fiber," Appl. Phys. Lett. **102**(20), 201107 (2013).
25. D. Radnatarov, S. Khripunov, S. Kobtsev, A. Ivanenko, and S. Kukarin, "Automatic electronic-controlled mode locking self-start in fibre lasers with non-linear polarisation evolution," Opt. Express **21**(18), 20626–20631 (2013).
26. J. P. Gordon, "Theory of the soliton self-frequency shift," Opt. Lett. **11**(10), 662–664 (1986).
27. S. M. Kobtsev and S. V. Smirnov, "Modelling of high-power supercontinuum generation in highly nonlinear, dispersion shifted fibers at CW pump," Opt. Express **13**(18), 6912–6918 (2005).
28. A. Aalto, G. Genty, and J. Toivonen, "Extreme-value statistics in supercontinuum generation by cascaded stimulated Raman scattering," Opt. Express **18**(2), 1234–1239 (2010).
29. X. M. Liu, L. R. Wang, D. Mao, and L. N. Duan, "Supercontinuum generation in standard single-mode fiber pumped by a nanosecond-pulse laser," Laser Phys. **22**(1), 227–231 (2012).
30. K. Yin, B. Zhang, W. Yang, H. Chen, and J. Hou, "Over an octave cascaded Raman scattering in short highly germanium-doped silica fiber," Opt. Express **21**(13), 15987–15997 (2013).
31. A. Zaytsev, C. H. Lin, Y. J. You, C. C. Chung, C. L. Wang, and C. L. Pan, "Supercontinuum generation by noise-like pulses transmitted through normally dispersive standard single-mode fibers," Opt. Express **21**(13), 16056–16062 (2013).
32. Y. Qiu, Y. Q. Xu, K. Y. Wong, and K. K. Tsia, "Enhanced supercontinuum generation in the normal dispersion pumping regime by seeded dispersive wave emission and stimulated Raman scattering," Opt. Commun. **325**, 28–34 (2014).
33. M. Liao, X. Yan, W. Gao, Z. Duan, G. Qin, T. Suzuki, and Y. Ohishi, "Five-order SRSs and supercontinuum generation from a tapered tellurite microstructured fiber with longitudinally varying dispersion," Opt. Express **19**(16), 15389–15396 (2011).

1. Introduction

Fiber lasers mode-locked due to non-linear polarisation evolution (NPE) demonstrate a unique diversity of mode-locked regimes [1–12], including both those featuring trains of pulse sets (soliton molecules and similar) and regimes with only one pulse on the cavity round trip. In the latter case, the laser can generate both fully and partially coherent pulses (the latter resembling pulse packets more than single pulses). The temporal intensity distribution of fully coherent pulses has a smooth envelope and is characterised by one temporal parameter, the envelope width (we will henceforth refer to these pulses as 'single-scale pulses'). The temporal intensity distribution of partially coherent pulses is stochastic: within a packet with duration of several to tens of picoseconds, there are faster stochastic intensity variations on the scale of 100 to several hundred femtoseconds. Correspondingly, the temporal intensity distribution of such pulses is described by two temporal parameters, the packet envelope width and the period of fast intensity fluctuations inside the train (such pulses will be hereafter referred to as 'double-scale' pulses). Double-scale pulses generated in fiber master oscillators passively mode-locked due to both NPE and other mechanisms do not yet have a universally accepted appellation. They are termed differently in various publications: noise-like pulses [13–15], double-scale lumps [16], femtosecond clusters [17], and so forth. These pulses may be interpreted as pulses contain a large number of femtosecond sub-pulses with different amplitude and phase [17]. These pulses can be readily identified in experiment by a distinct shape of auto-correlation function containing a narrow (100–300 fs) peak on a picosecond pedestal.

The current interest in these pulses is predominantly due to their having femtosecond-scale partials with high peak intensity, even though the fiber laser cavity may have relatively high dispersion. They are furthermore attractive because this type of pulses is most likely to be generated in long cavities [18, 19] and they may deliver record-high energy (for mode-locked lasers) immediately at the output of a master oscillator without Q-switching or additional amplification.

The issue of double-scale pulse applications is currently being actively explored. Article [17] demonstrated the advantages of these pulses in laser-induced breakdown spectroscopy. It

#214558 - $15.00 USD Received 23 Jun 2014; accepted 7 Aug 2014; published 20 Aug 2014

was shown in [20] that double-scale pulses may be efficiently transformed into second-harmonic radiation. The present study was focused on Raman scattering of single- and double-scale fiber laser pulses in a long extra-cavity fiber. As it is illustrated in the following sections, cascaded SRS spectra given rise by radiation of these pulses exhibit substantial differences, even though the temporal envelopes of single- and double-scale pulses have similar widths. Additionally, the character of temporal broadening of single- and double-scale fiber laser pulses in a long extra-cavity fiber is also different.

It should be emphasised that earlier studies of Raman scattering of laser pulses in long fibers [21–24] did not compare spectral and temporal pulse shape transformation of single- and double-scale pulses in a long extra-cavity fiber. This work draws such a comparison for the first time. Furthermore, here we study for the first time cascaded SRS of picosecond pulses in ultra-long extra-cavity phosphosilicate-glass fiber.

2. Experimental setup

Generation of single- and double-scale pulses was performed in the fiber-optical system outlined in Fig. 1. Double-clad Yb-fiber pumped with a diode laser through a beam combiner at 975 nm was used as the active medium of the master oscillator. Unidirectional operation of the laser's ring cavity was ensured by an optical isolator and a polarisation beam splitter was used to couple radiation out of the cavity. To simplify and speed up alignment of the laser for different mode locking regimes, in which single- or double-scale pulses could be generated, two intra-cavity polarisation controllers were installed, even though we earlier showed [25] that only one such controller may be necessary to trigger mode-locked operation.

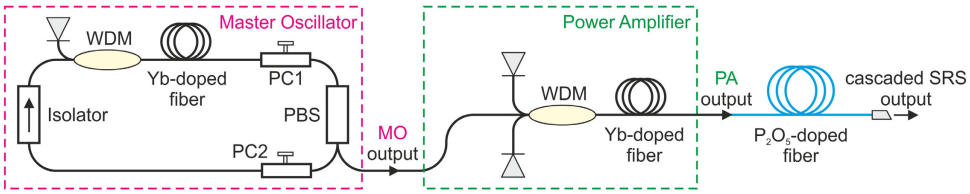

Fig. 1. Experimental layout: PC1, PC2 – polarisation controllers, WDM – fiber spectral combiner, MO – master oscillator, PA – power amplifier.

To determine which specific generation regime was realised, output radiation spectra and pulse auto-correlation function were measured. Typical spectra and auto-correlation functions of generated single- and double-scale pulses are presented in Fig. 2.

Pulse repetition rate was 14 MHz and duration of single-scale pulses was 3 ps, while the width of the temporal envelope of double-scale pulses did not exceed 8.5 ps. The average output power in both regimes amounted to approximately 20 mW. In order to generate broad Raman scattering spectra, the output of the fiber master oscillator was boosted in a fiber amplifier to the average level of 840 mW. The amplified radiation was guided into a 1.2 km long commercially available phosphosilicate-glass fiber with the core diameter of 6 μm. Spectral parameters of the radiation were controlled with an optical spectrum analyser (Ando AQ6370), while temporal ones were registered with an auto-correlator (FS-PS-Auto, 10 fs – 40 ps), photo-detector and oscilloscope with resolution of ~40 ps.

#214558 - $15.00 USD Received 23 Jun 2014; accepted 7 Aug 2014; published 20 Aug 2014

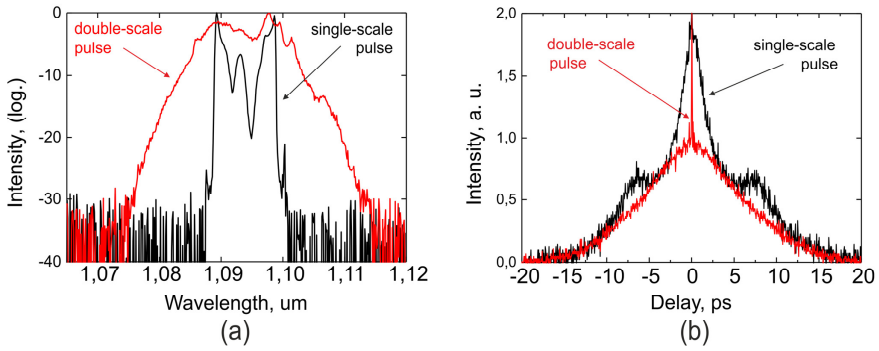

Fig. 2. (a) Radiation spectra of single-scale (black curve) and double-scale (red curve) pulses at the output of the master oscillator; (b) Auto-correlation functions of single-scale (black curve) and double-scale (red curve) pulses at the output of the master oscillator.

3. Results

Figure 3 compares SRS spectra of single- and double-scale pulses after passing through a long P_2O_5-doped silica fiber at different average input powers.

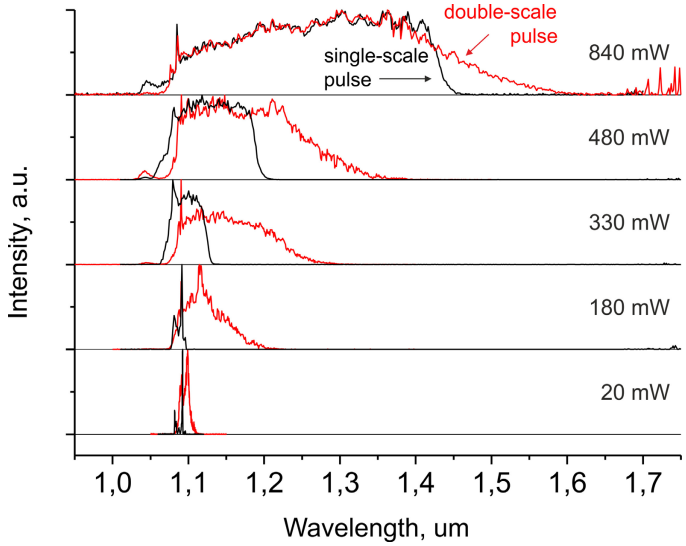

Fig. 3. Cascaded SRS spectra of single-scale (black curves) and double-scale (red curves) pulses. The average radiation power at the input of the P_2O_5-doped silica fiber is specified at the right.

At the lowest average radiation power of 20 mW, spectra at the output of phosphosilicate-glass fiber almost exactly reproduce the original spectra generated by master oscillator. At higher average radiation powers, spectral broadening occurs towards longer wavelengths, leading us to attribute it to Raman scattering. It can be seen that at intermediate power levels (up to 500–600 mW) Raman scattering spectra of double-scale pulses are substantially wider than analogous spectra of single-scale pulses. The spectra also differ in shape. Thus, at low pump powers broadened spectra of single-scale pulses are much more symmetrical, indicating that self-phase modulation contributes considerably to spectral broadening in this case. As average power increases up to 500 mW, spectra of single-scale pulses become more and more asymmetrical and broaden mainly towards longer wavelengths, while remaining quasi Π-shaped. In contrast, spectra of double-scale pulses contain a sloping long-wavelength wing and a distinct peak at 1090 nm corresponding to residual pump radiation, which did not

#214558 - $15.00 USD Received 23 Jun 2014; accepted 7 Aug 2014; published 20 Aug 2014

undergo Raman scattering. Both features of double-scale pulse spectra may be attributed to different statistics of such pulses. Whereas single-scale pulses are smooth and uniformly broadened, double-scale pulses contain different quasi-random components with different wavelengths and intensity. Some of these components may have very high (up to an order of magnitude higher than average) power, which results in higher efficiency of Raman conversion and larger frequency red-shifts. However, the portion of such relatively high-intensity components is much smaller compared to single-scale pulses (see Fig. 4(a)). Indeed, whereas $sech^2$ pulses have 50% of their energy stored in an area with instantaneous power P higher than 75% of peak power P_{max}, according to our simulations similar to [20], double-scale pulses have in the same area only about 8% of their energy (note that exact values may vary for different lasing regimes [20]). This leads to higher Raman frequency shifts of double-scale pulses and to formation of sloping (low-intensity) long-wavelength spectral wings in the process of spectral broadening of such pulses.

As the average input power grows above 800 mW, Raman scattering spectra of single-and double-scale pulses approach each other both in shape and in width. This indicates that initial pulse structure ceases to play a significant role when considerable (more than by 200-300 nm) spectral broadening takes place which corresponds to energy transfer into anomalous dispersion region with further pulse decay due to modulation instability and evolving solitonic effects in spectral broadening. Let's note, however, that the long-wavelength wing of spectra produced by single-scale pulses contains separate peaks similar to self-frequency-shifted solitons [26] whereas analogous spectral wing produced by double-scale pulses is much smoother and gentler sloping. The latter fact may be also attributed to partially coherent nature of double-scale pulses that leads to spectral smoothing due to averaging over optical spectral analyser registration time similar to previous finding for CW-pumped supercontinuum [27]. Relatively smooth radiation spectra observed at high average input powers represent supercontinua composed of several spectral SRS Stokes components. Analogous mechanism of supercontinuum generation was earlier discovered in germanosilicate-glass [22, 28–32] and micro-structured fibers [33]. It is necessary to note that smoothing out of the output spectrum in the present work took place directly within the phosphosilicate-glass fiber: we only registered the radiation spectrum at the input and output of the amplifier and did not monitor any evolution of spectrum inside at all radiation power levels. In [22], broadening of the pulse spectrum during amplification facilitated leveling out spectral dips between peaks of neighbouring Stokes components. However in this work, no spectral broadening of input pulses took place inside the amplifier, and the resulting output spectrum formed by a combination of several spectral SRS Stokes components was smoothed out due to relatively broad initial radiation spectra of single- and double-scale pulses. Thus, spectral width of single-scale pulses exceeded 15 nm, and that of double-scale pulses was broader than 20 nm.

We chose P_2O_5-doped silica fiber for these experiments expecting significant conversion of the input pulse energy into Stokes components around 1240 and 1480 nm in P_2O_5. However, as the experimental results demonstrate, the measured spectra do not have noticeable features around these wavelength values and are, as a whole, formed due to superposition of radiation spectra of multiple Stokes components generated by SRS in the germanosilicate host of the selected fiber.

In Fig. 4(b) and 4(c) temporal distributions of radiation intensity of single- and double-scale pulses are shown at the output of the long extra-cavity fiber at different average input powers. Since quite a long section of phosphosilicate-glass fiber was used in our experiments (which is estimated an order of magnitude longer than the length of effective non-linear interactions for laser pulses), temporal intensity distributions registered at fiber exit are associated with spectral profiles. Thus, pulse duration after propagation through the phosphosilicate-glass fiber grows for both types of pulses from 0.5 to 1 up to 5.5–6 ns along with spectral width as pulse power is increased from 55 to 400 mW. A remarkable feature of spectrally-broadened double-scale pulses clearly visible in Fig. 4(c) is represented by a distinct narrow peak close to the trailing edge of the pulse, which is directly related with a

#214558 - $15.00 USD Received 23 Jun 2014; accepted 7 Aug 2014; published 20 Aug 2014

spectral peak at 1090 nm and corresponds to residual pump radiation. (Note that at the lowest average power of 55 mW there is a peak at the leading edge of the pulse corresponding to the peak at the long-wavelength edge of the spectrum shown in Fig. 3 for the lowest power level). Duration of this peak is about 200 ps, which corresponds to spectral broadening of a 17-nm wide spectrum after propagation through the fiber with dispersion D ~40 ps^2/nm/km.

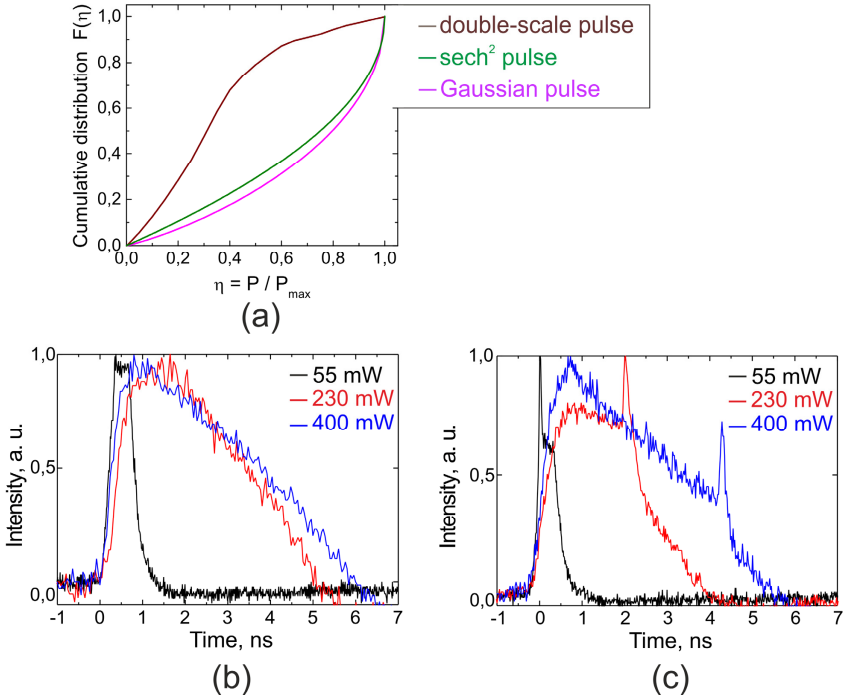

Fig. 4. (a): Simulated power statistics for double-scale and single-scale ($sech^2$ and Gaussian pulse): fraction of pulse energy stored in parts of pulse where instantaneous power P related to max (peak) power P_{max} is less than η. Figure 4(b) and 4(c): Temporal intensity distribution of single-scale (b) and double-scale (c) pulses at the output of the long extra-cavity fiber at different average input powers (shown at upper right-hand corners).

3. Conclusion

The difference in efficiency of non-linear transformation of single- and double-scale pulses that we observed earlier [20] also manifested itself in the present work in cascaded SRS of these pulses. Similar to [20], double-scale pulses demonstrated their relatively better efficiency of non-linear transformation, but this time also in cascaded SRS. High efficiency of non-linear conversion of double-scale pulses, which are often termed 'noise' or 'stochastic' and which were earlier not considered for practical applications, stimulates further studies of practical applications of radiation pulses, which may deliver record-high energy directly at the output of fiber master oscillators [6].

Acknowledgments

This work was supported by the Grants of Ministry of Education and Science of the Russian Federation (agreement No. 14.B25.31.0003, ZN-06-14/2419, order No. 3.162.2014/K); Russian President Grant MK-4683.2013.2; Grant of SKOLKOVO Foundation (G-13-131); Council of the Russian President for the Leading Research Groups (project No. NSh-4447.2014.2).